Received: 5 April 2021 | Revised: 9 September 2021 | Accepted: 30 September 2021

IET Renewable Power Generation

DOI: 10.1049/rpg2.12313

The Institution of Engineering and Technology WILEY

ORIGINAL RESEARCH PAPER

Impact assessment framework of PV-BES systems to active distribution networks

Kalliopi D. Pippi[1] | **Theofilos A. Papadopoulos**[1] | **Georgios C. Kryonidis**[2]

[1] Power Systems Laboratory, Department of Electrical and Computer Engineering, Democritus University of Thrace, Xanthi, Greece

[2] Electrical Machines Laboratory, School of Electrical & Computer Engineering, Aristotle University of Thessaloniki, Thessaloniki, Greece

Correspondence
Theofilos A. Papadopoulos, Department of Electrical and Computer Engineering, Democritus University of Thrace, Kimmeria Campus, 67100 Xanthi, Greece.
Email: thpapad@ee.duth.gr

Funding information
Hellenic Foundation for Research and Innovation, Grant/Award Number: HFRI-FM17-229; Hellenic Foundation for Research and Innovation (H.F.R.I.)

Abstract

Passive distribution networks tend to become active, due to the high penetration of photovoltaic units, battery energy storage utilization and their combined active participation to distribution network operation. In this paper, a framework for the assessment of the impact of photovoltaic and battery energy storage systems on voltage profiles, power losses and reverse power flow phenomena of active distribution networks is proposed. Also, the utilization of photovoltaic and battery energy storage systems is evaluated. The proposed methodology is applied to statistically analyse results obtained from annual timeseries power flow calculations in a real 18-bus low-voltage network over a range of operating conditions; the obtained results are quantified using a set of probabilistic indices. The proposed framework can be a useful tool for distribution system operators to identify operational challenges and ensure the optimal exploitation of end-user and network assets.

1 | INTRODUCTION

The need for clean and sustainable power becomes more critical than ever due to the negative environmental impact of the conventional power plants. For this reason, in the last decades, the installation of distributed generation (DG), and especially photovoltaics (PVs) in the low-voltage (LV) distribution network has been significantly increased leading to the gradual conversion of the conventional passive distribution networks to active ones [1]. In particular according to [2], active distribution networks (ADNs) are "*distribution networks with a significant amount of distributed generation (DG) which at specific periods of time (e.g. at minimum loading conditions) is a net exporter of active power, but at other times (e.g. at maximum loading conditions) may be a net importer of active power*". In this context, DGs can contribute to reduced network power losses, voltage profile improvement and participate in the distribution network operation by providing ancillary services [3,4]. Nevertheless, the increasing penetration of DGs in ADNs poses unprecedented technical challenges to the network operators, jeopardizing the reliable operation of power systems, for example, power fluctuations [5], voltage rise [6,7] and network component overloading [8].

Therefore, the systematic evaluation of the impact of DG units on the performance of ADNs is very important. For this purpose, index-based approaches have been proposed to quantify the impact of DG units on the critical operating parameters of ADNs. Specifically, in [9] the technical benefits of DG incorporation regarding voltage profiles, line losses and environmental reduction are quantified by employing a set of probabilistic indicators. In [10] an index-based methodology is proposed to correlate reverse power flow (RPF) incidents to voltage limit violations. In [11], a comprehensive framework is presented to assess the effect of residential PVs on a real LV network. The framework utilizes a set of technical indicators regarding voltage violations and network congestion phenomena to identify the most cost-effective grid reinforcement investment ensuring the reliable grid operation. However, both [10] and [11] investigate only three-phase balanced networks. Furthermore, in [12,13] a set of indices is proposed to evaluate the impact of net-zero energy buildings (NZEBs) on the performance of the electricity grid.

Moreover, the rapidly developing battery energy storage (BES) technology [14] at the residential level, alongside PV systems, can improve the household selfsufficiency and provide a variety of ancillary services [15]. In the relevant literature,

several papers [16–20] can be found, investigating the impact of PV-BES systems on the performance of ADNs. In [16], the effect of roof-top solar PVs and residential BES systems on a South African LV network is examined to identify the least penetrative size of units improving the technical and economic performance of the utility grid and end-users. In [17], a methodology is proposed to evaluate the impact of PV-BES on power losses and voltage profiles in an Australian LV network. Nevertheless, in both the above analyses, there are no technical indices utilized to systematically quantify the benefits of residential PV-BES systems. In [18], the impact of varying capacity sizes of BES systems on load matching capabilities of residential prosumers is investigated utilizing well-known load matching indicators. However, the impact of BES on grid parameters is not evaluated. In [19], the effect of BES and PV systems operation is examined employing a voltage stability and quality index. In addition, in [20], apart from the systematic evaluation of network voltages using performance indicators, the power flow through network elements is also assessed. Although, both [19,20] focus on the analysis of the network performance; the effect of BES utilization on LV prosumers is not considered.

According to the above analysis, it can be deduced that literature lacks a comprehensive methodology to investigate different technical aspects emerged in modern LV networks, both from the end-user's and also from the system operator's perspective. This paper aims to fill this gap by introducing a generalized framework for the impact assessment of PV-BES systems on both end-users' behaviour and the operation of ADNs. The proposed framework is generalized in the sense that it can be applied to any LV network regardless of its configuration, operating conditions, PV and/or BES system control strategies etc. In particular, the main strengths and contributions are summarized below:

1. The proposed framework involves statistical analysis of technical indices calculated by performing timeseries power flow simulations on annual basis. Furthermore, a set of probabilistic indices is introduced to evaluate the load matching capabilities and PV-BES system utilization of end-users (end-user-oriented analysis) as well as to quantify the impact of PV-BES systems on the network performance, in terms of voltage profiles, power losses and RPF incidents (network-oriented analysis). The proposed indices are partly adopted from literature and modified in a probabilistic manner, or mostly new ones are developed based on a previous study of the authors [21].
2. The proposed approach can constitute a generalized tool useful for both end-users and system operators. Specifically, end-user analysis can be used to investigate the integration of PV-BES systems and evaluate different types of demand-side measures [22]. Network-oriented analysis can provide valuable information during the network planning phase by identifying operational challenges and ensure the optimal exploitation of network assets on the basis of PV-BES system control strategies.

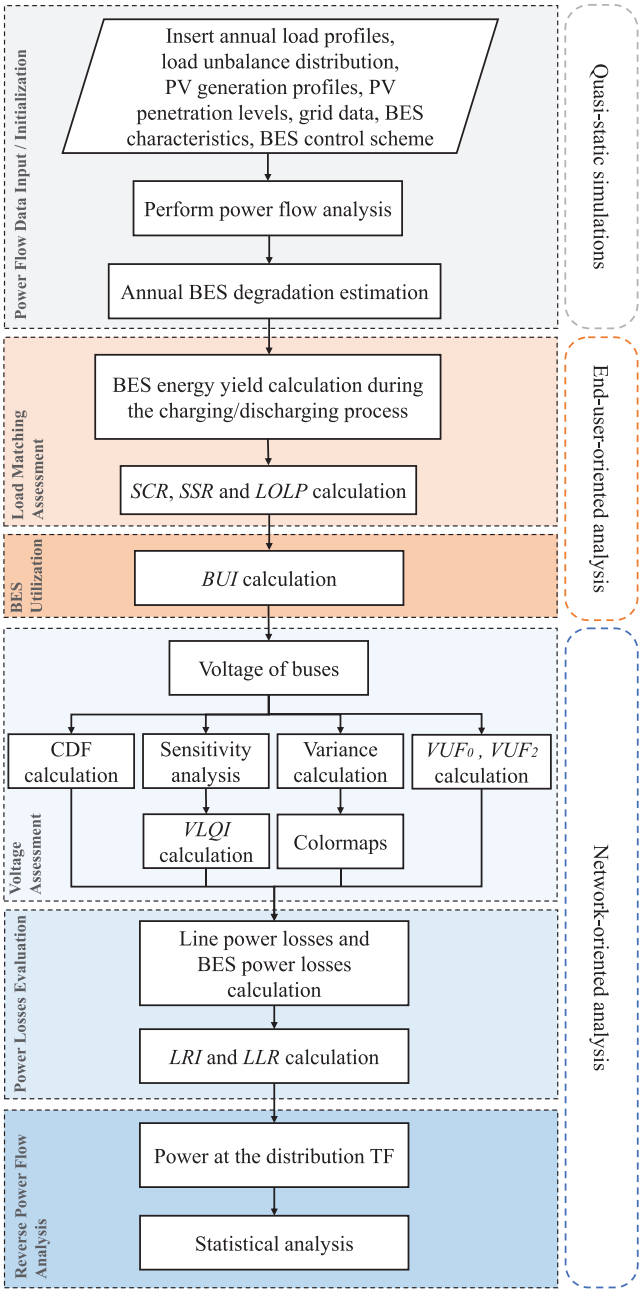

FIGURE 1 Flowchart of the proposed methodology

The rest of the paper is organized as follows: In Section 2, the proposed methodology and evaluation indices are presented. The simulation model and the examined network operating scenarios are described in Sections 3 and 4, respectively. Results are analysed and discussed in Section 5. Finally, Section 6 summarizes the most important remarks of this work.

2 | METHODOLOGY

The proposed framework is depicted in the flowchart of Figure 1. The core of the methodology is the statistical

analysis of the results and the evaluation indices obtained on the basis of quasi-static analysis of LV ADNs. This involves the following main steps:

1. Quasi-static simulations: timeseries power flow analysis is conducted by using annual load and PV production timeseries; different scenarios and end-user operating conditions are considered. The annual timeseries of power demand and PV production, the grid configuration as well as the required parameters regarding the operating scenario are used as inputs to the power flow problem. In this step, BES system degradation is also estimated.
2. End-user-oriented analysis: this analysis focuses on the evaluation of the end-users and the corresponding PV-BES system performance. This is achieved by calculating three load matching indices proposed in the relevant literature as well as by introducing a new index regarding BES system utilization. In this step, BES degradation is also evaluated.
3. Network-oriented analysis: the impact of the examined scenarios on the grid operation is assessed by analysing the calculated voltage levels, power losses and active or reactive power flows at the distribution transformer. In particular, voltage assessment is performed in terms of voltage magnitude results as well as of a set of probabilistic indices. The impact of PV-BES systems on the ADN power losses is investigated in terms of decomposition to distribution line and BES losses. Finally, RPF incidents are examined by means of statistical analysis.

All steps of the proposed framework are described in detail in the following subsections.

2.1 | End-user-oriented analysis

Different indices have been proposed to evaluate the sizing of PV systems according to the end-user's load profile [23]. However, the everincreasing installation of BES systems necessitates revisiting the existing indices describing their load matching capabilities [23]. In this context, the revisited self-consumption rate (*SCR*) is defined in (1) to evaluate the PV produced energy that is directly consumed on-site or stored in the BES system [23].

$$SCR\ (\%) = \frac{C + E}{B + C + D}. \tag{1}$$

Accordingly, to assess the load energy covered by the PV production and the BES stored energy, the revisited self-sufficiency rate (*SSR*) index is used [23]:

$$SSR\ (\%) = \frac{C + E}{A + C + E + F}. \tag{2}$$

Here, as it is shown in Figure 2, A and F denote the load energy covered by the grid, B and C indicate the excess of the PV produced energy and the self-consumed energy, respectively; D and E stand for the surplus PV energy stored in the BES and the energy supplied to the load by the BES, respectively.

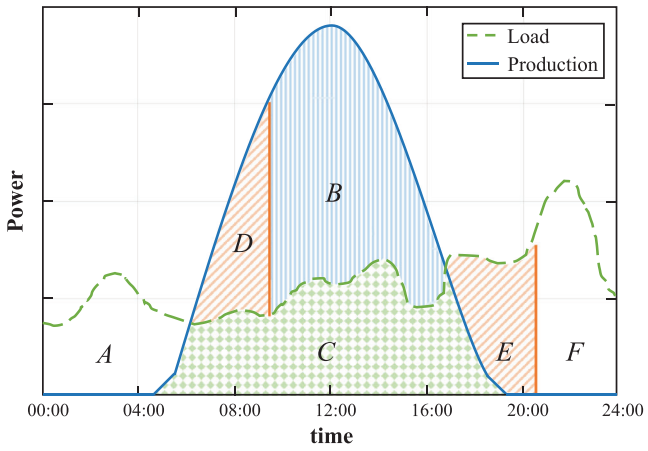

FIGURE 2 Daily power profiles of typical PV-BES prosumer

SCR and *SSR* can be used to qualitatively evaluate the PV production share [22]. Considering quantitative analysis, the loss of load probability (*LOLP*) is adopted, expressing the percentage of time ($t_{P_{net}>0}$) that the PV and BES system do not cover load demand [22]; *LOLP* is calculated as:

$$LOLP\ (\%) = \frac{t_{P_{net}>0}}{T}, \tag{3}$$

where P_{net} is the netted power at the prosumer's bus and T is the time under consideration. Note that, if P_{net} is positive, the PV-BES prosumer consumes energy from the grid.

To specifically evaluate the performance of the BES system, the battery utilization index (*BUI*) is introduced; *BUI* is the ratio of the annual energy yield ($E_{\mathrm{ch/disch}}$) during BES charging/discharging process to the annual energy yield (E_{rated}) on the basis of BES rated characteristics, as shown in (4):

$$BUI\ (\%) = E_{\mathrm{ch/disch}} / E_{\mathrm{rated}}, \tag{4}$$

where $E_{\mathrm{ch/disch}}$ and E_{rated} are calculated by (5) and (6).

$$E_{\mathrm{ch/disch}}\ (\mathrm{kWh}) = \sum_{k=1}^{8760} E_{\mathrm{oper}}^{\mathrm{ch/disch}}\ (k), \tag{5}$$

$$E_{\mathrm{rated}}\ (\mathrm{kWh}) = 365 \cdot E_{\mathrm{max}} \cdot DoD, \tag{6}$$

where E_{oper} is the charging/discharging energy during the BES operation, *DoD* is the maximum depth of discharge, and E_{max} is the maximum energy content (capacity) of the BES.

2.2 | Network-oriented analysis

Initially, as a general assessment of the network voltage performance, the voltages at buses, where end-users are connected,

are statistically analysed by using cumulative distribution functions (CDFs). The scope of this analysis is to identify general trends in the overall system performance. In this context, the voltage level quantification index (*VLQI*) is also adopted, to systematically quantify the impact of the PV/PV-BES systems. The *VLQI* was originally introduced in [9]. Nevertheless, the implementation therein assumes that all network buses are of the same importance, which is not valid in real distribution networks. To consider the behaviour of the most critical network buses accordingly, the *VLQI* is modified by introducing sensitivity theory. Moreover, the *VLQI* is extended to be applied for statistical analysis. The proposed probabilistic *VLQI* is defined as:

$$VLQI = \frac{1}{8760} \cdot \sum_{k=1}^{8760} \frac{\left(\sum_{n=1}^{N} v_n(k)\, w_n\right)_{\text{ADN(PV/PV-BES)}}}{\left(\sum_{n=1}^{N} v_n(k)\, w_n\right)_{\text{Passive}}}, \quad (7)$$

where k is the discrete time step, N is the number of network buses, v_n is the normalized positive-sequence voltage at bus n and w_n is the sensitivity of bus n with respect to active power variations of the same bus ($\partial V_n/\partial P_n$); it is derived by means of (8) [6]:

$$\begin{bmatrix}\Delta\delta\\ \Delta V\end{bmatrix} = J^{-1}\begin{bmatrix}\Delta P\\ \Delta Q\end{bmatrix} = \begin{bmatrix}\left(\frac{\partial\delta_n}{\partial P_n}\right)_{N\times N} & \left(\frac{\partial\delta_n}{\partial Q_n}\right)_{N\times N}\\ \left(\frac{\partial V_n}{\partial P_n}\right)_{N\times N} & \left(\frac{\partial V_n}{\partial Q_n}\right)_{N\times N}\end{bmatrix}\begin{bmatrix}\Delta P\\ \Delta Q\end{bmatrix}. \quad (8)$$

Here, $\mathbf{J}^{-1}$ is the inverse $2N \times 2N$ Jacobian matrix with elements, the partial derivatives, $(\frac{\partial\delta_n}{\partial P_n})_{N\times N}$, $(\frac{\partial\delta_n}{\partial Q_n})_{N\times N}$, $(\frac{\partial V_n}{\partial P_n})_{N\times N}$and $(\frac{\partial V_n}{\partial Q_n})_{N\times N}$; $\boldsymbol{\Delta V}$ is the voltage magnitude and angle ($\boldsymbol{\Delta\delta}$) variations with respect to active ($\boldsymbol{\Delta P}$) and reactive ($\boldsymbol{\Delta Q}$) power changes. Alternatively, for the calculation of w_n a simplified approach can be adopted [24]:

$$w_n = -\frac{1}{V_{\text{nom}}} \sum_{ab\in[TF^{sd},n]} R_{ab}, \quad (9)$$

where V_{nom} is the nominal network voltage at the end-user's side and R_{ab} is the total resistance of the path ab, connecting the secondary of the distribution transformer to bus n. Note that, in (7) the numerator corresponds to ADN operation, that is, end-users with PV or PV-BES systems, while the denominator to passive operation.

Voltage sensitivity can be also studied on the basis of $\sigma^2_{n,h}$, the mean voltage variance index. $\sigma^2_{n,h}$has been introduced to statistically analyse voltage variations during the day; it is defined for each network bus as:

$$\sigma^2_{n,h} = \frac{1}{D-1}\sum_{d=1}^{D}\left|V_n(d,h) - \bar{V}_n(h)\right|^2, \quad (10)$$

where D is the total number of days, that is, 365, $V_n(d,h)$ is the voltage magnitude of bus n at day d and hour h, while $\bar{V}$(h) is the annual mean voltage for hour h. It should be noted that, by using w_n and $\sigma^2_{n,h}$ the most critical buses, in terms of sensitivity to voltage changes can be identified. In this sense, the network operators can target their analysis to these buses, instead of performing network global assessment.

Furthermore, to evaluate the severity of the voltage unbalance caused by single-phase or unbalanced loads, a set of indices is used; it contains the zero- and negative-sequence voltage unbalance factors, defined by (11) and (12), respectively [25].

$$VUF_0(\%) = \frac{V_0}{V_1}\cdot 100\%, \quad (11)$$

$$VUF_2(\%) = \frac{V_2}{V_1}\cdot 100\%, \quad (12)$$

where V_0, V_1 and V_2 are the zero-, positive- and negative-sequence voltages, respectively.

For the evaluation of the effect of the PV-BES operation on the total ADN power losses, the losses reduction index (*LRI*) and the losses to load ratio (*LLR*), defined in (13) and (14), respectively, are used.

$$LRI(\%) = \frac{\Sigma P_{\text{Losses(ADN)}}}{\Sigma P_{\text{Losses(PassiveNetwork)}}}, \quad (13)$$

$$LLR(\%) = \frac{\Sigma P_{\text{Losses(ADN)}}}{\Sigma P_{\text{Load}}}, \quad (14)$$

where $\Sigma P_{\text{Losses(ADN)}}$ and $\Sigma P_{\text{Losses(PasssiveNetwork)}}$are the system losses (line and BES system losses) for ADN and passive network operation, respectively; $\Sigma P_{\text{Load}}$is the total load demand. Both indices can be used to determine the optimal PV penetration level in terms of minimum system losses. Note that, *LRI* and *LLR* were originally proposed to evaluate the impact of DGs on distribution networks [9,26]. In this work, *LRI* and *LLR* are modified to analyse PV-BES prosumers; thus, apart from line losses, BES losses are also included in (13) and (14).

Finally, increased DG penetration in LV grids may result in undesired RPF in terms of upstream network power flows. Therefore, the analysis of active or reactive power at the secondary of distribution transformers can provide valuable information to the system operator to identify possible cases of RPF, assess their severity and ensure the reliable operation of the grid without violating technical limitations.

In this regard, Quantile-Quantile (Q-Q) plots are used. A Q-Q plot is a graphical method for determining whether two sets of sample data, for example., Q_1 and Q_2, correspond to the same distribution, by plotting their quantiles against each other. If the compared distributions are similar, the samples in the Q-Q plot follow a linear pattern, that is, $y = x$. This implies that, Q-Q plots can be used as graphical means to analyse the shape of the data distribution and extract statistical measures [27]. In this sense, the impact of different operating scenarios on the power flow at the distribution transformer is systematically assessed by

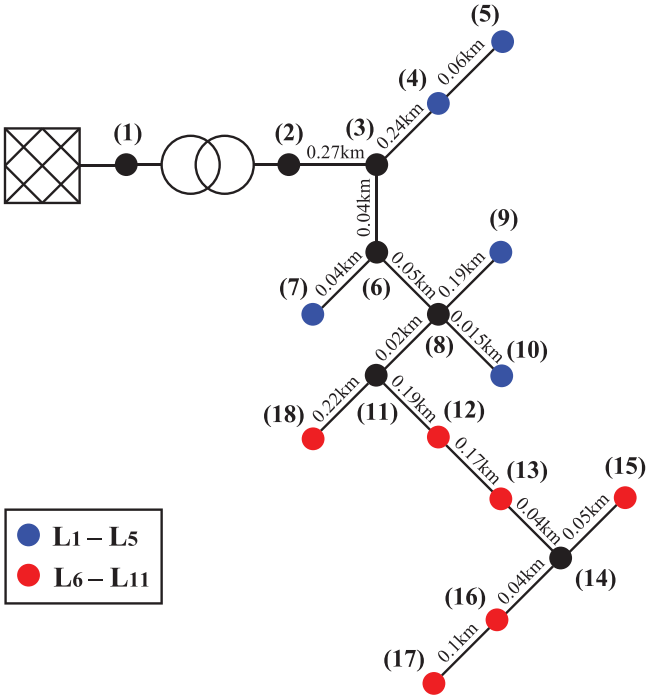

FIGURE 3 Single-line diagram of the ADN

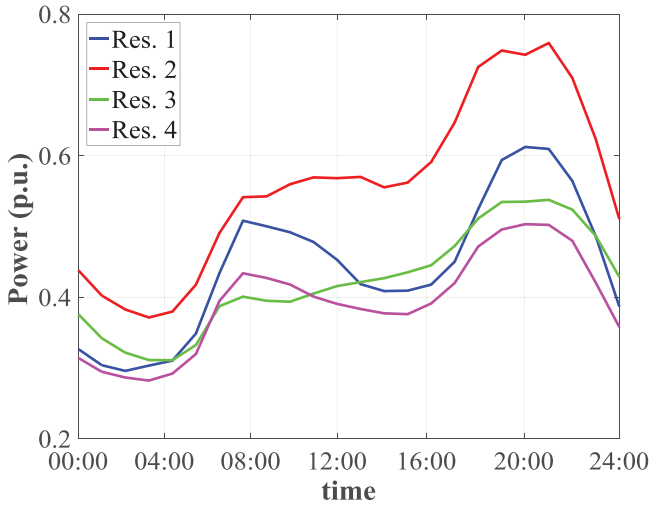

FIGURE 4 Daily average profile patterns of each load class

investigating the similarities or differences between the corresponding active power data.

3 | SIMULATION MODEL

In this section, the input data of the proposed framework, that is, the test network, the load and PV production data, the BES characteristics and control strategies, as well as the modelling of the BES are described. The simulation model and used data are available in [28].

3.1 | System under study

Annual timeseries simulations of 1-h resolution (8760 samples) are conducted in the Open Distribution System Simulator (OpenDSS) software. OpenDSS is an open-source multipurpose distribution system analysis tool and it is mainly utilized to solve the power flow problem in power systems employing an iterative power flow algorithm, namely the "Current Injections Mode" [29]. Data postprocessing of the timeseries has been applied to remove possible corrupted measurements, caused by instrument failures, communication errors or telemetry loss. The single-line diagram of the examined ADN is depicted in Figure 3. Note that, the number in the brackets denotes the network bus number. The examined ADN is a radial three-phase LV network with a base frequency 50 Hz, consisting of 18 buses and a 630 kVA, 20 kV/0.69 kV delta-wye distribution transformer. The positive- and zero-sequence line impedances are: $Z_1 = 0.215 + j0.334\ \Omega/km$ and $Z_0 = 0.363 + j1.556\ \Omega/km$, respectively. The ADN consists of 11 three-phase residential end-users classified into two main groups, that is, Group #1 and Group #2. Group #1 contains end-users L_1–L_5 (denoted with blue), each of 15.66 kVA rated apparent power (S) and power factor (pf) 0.96 lagging; Group #2 corresponds to L_6–L_{11} (denoted with red), each of $S = 9.49$ kVA and $pf = 0.95$.

3.2 | Load timeseries

Annual residential electricity profiles from the National Renewable Energy Laboratory (NREL) dataset are used. Specifically, electricity data of the West Coast region of USA are selected, since this region presents high resemblance to the Mediterranean climate [30]. Load data of 2528 households are categorized into four main load classes, namely Res. 1–4. By averaging the annual profiles of the end-users belonging to the same load class, the representative (mean) annual profile (8760 samples) of the load class is obtained. Each of the load classes is then normalized based on the corresponding maximum power and the normalized timeseries is generated. For ease of simplicity the daily profile (24 samples) of each load class, based on the normalized timeseries, is plotted in Figure 4 as the average of the samples corresponding to the same time interval of the day.

3.3 | PV timeseries

The annual PV timeseries are obtained by the online simulation tool of [31], allowing to perform calculations of the hourly power output of PV systems. The PV model input is the hourly incident solar irradiation for 35° tilt and 180° azimuth of PV modules located in the region of Xanthi, Greece; the generated power is calculated, assuming 10% PV system losses and PV size 1 kWp, corresponding to 1 p.u. base. In Figure 5 the average daily profile of PV production in p.u. is presented.

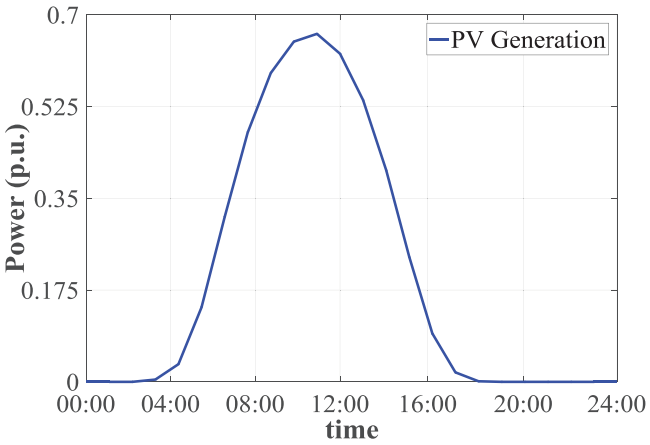

FIGURE 5 Average daily production profile

Algorithm 1 BES CS1

1: **if** $P_{load} \geq P_{PV}$
2: BES discharges
3: **else**
4: BES charges
5: **end if**

Algorithm 2 BES CS2

1: **if** $P_{PV} \geq 0.7 \cdot P_{PV\,nominal}$
2: BES charges
3: **else if** $P_{PV} = 0$
4: BES discharges
5: **end if**

3.4 | BES modelling

Each ADN prosumer can also employ a BES system. The BES modelling is described by the energy content (E) at each time instant t, given in (15):

$$E(t) = E(t-1) + \eta_c \cdot P_c(t) \cdot \Delta t - \frac{1}{\eta_d} \cdot P_d(t) \cdot \Delta t, \quad (15)$$

where Δt is the time step, P_c and P_d are the BES charging and discharging power, respectively; η_c and η_d are the corresponding charging and discharging BES efficiency.

In addition, the aging model proposed in [32] is used to estimate according to (16) the capacity degradation of lithium-ion BES under different control strategies (CSs).

$$capd^p = 1 - \alpha e^{-\beta \cdot f_d} - (1-\alpha)\, e^{-f_d}. \quad (16)$$

Here, $capd$ denotes the BES capacity degradation during time period p, α and β are parameters determined by experimental data and f_d is the degradation rate factor. The last parameter depends on: (a) the state of charge (SoC) of the BES, (b) the depth of discharge (DoD), (c) the BES temperature, (d) the calendar degradation rate and (e) the number of cycles over the BES system lifetime obtained by the rainflow counting algorithm [33].

Among a variety of BES CSs, two of the most well-established CSs are examined, namely CS1 and CS2. These CSs have been employed to demonstrate the application of the proposed assessment framework under specific network operating conditions. Nevertheless, the proposed framework is generalized, thus different types of BES control schemes, management strategies (aggregated or individual) and optimization techniques for BES utilization [34–36] can be incorporated to evaluate their effectiveness and applicability under different cases. The examined CSs are further discussed in detail:

BES CS1: This CS is widely used by prosumers to maximize their self-consumption. According to this CS, the BES charges when the load demand (P_{load}) is lower than the generated PV power (P_{PV}). Otherwise, the BES discharges. Algorithm 1 summarizes this procedure.

BES CS2: This strategy is designed by taking into account only the PV generated power. It is a common control scheme employed in Germany to avoid excessive PV production [37]. Specifically, when the generated power exceeds 70% of the nominal PV peak power ($P_{PV\,nominal}$), the BES starts charging. Otherwise, if there is no PV production, the BES discharges. This process is described by Algorithm 2.

The BES operation is constrained by its characteristics, depending on the technological type. The BES characteristics are also incorporated in the simulation model. Specifically, for Group #1 a 10 kWh lithium-ion manganese oxide (LMO) BES is assumed with characteristics: $P_c = P_d = 5$ kW, $\eta_c = \eta_d = 95\%$ and $DoD = 80\%$. Accordingly, for Group #2, a 6 kWh LMO BES is used with $P_c = P_d = 3$ kW, $\eta_c = \eta_d = 95\%$ and $DoD = 80\%$. Note that for both prosumer types, the BES are sized according to the corresponding end-user's demand. Specifically, the P_c and P_d are selected to cover 33% of the maximum load demand. Additionally, the BES power to energy ratio is considered equal to 50%.

4 | SIMULATION PROCEDURE

Several scenarios are performed and the effect of various parameters to the ADN performance is evaluated. The examined network operating scenarios are:

- Passive network (reference): all network LV end-users consume energy.
- PV ADN: all LV end-users are PV prosumers.
- PV-BES ADN: all LV end-users are PV-BES prosumers.

TABLE 1 Examined cases of BES parameters

		Capacity (kWh)		Power (kW)	
		Group		Group	
Case	Description	#1	#2	#1	#2
1	Reference case	10	6	5	3
2	Power decrease (50%)	10	6	2.5	1.5
3	Power increase (50%)	10	6	7.5	4.5
4	Capacity and power increase (50%)	15	9	7.5	4.5
5	Capacity and power increase (100%)	20	12	10	6

TABLE 2 Load allocation across three phases

Phase	Group #1	Group #2
A	40%	20%
B	35%	30%
C	25%	50%

At each scenario, the PV penetration level, that is, the percentage of the PV size to the load nominal apparent power at each bus as well as BES characteristics, that is, power and maximum energy content were assumed varying. The PV penetration ranges from 50% to 100%; the examined cases regarding the BES characteristics are described in Table 1. Note that, in all cases the same load and PV production timeseries is applied to all end-users.

Additionally, a set of simulations to assess network unbalance conditions are performed. In particular, Group #1 and Group #2 load is assumed being allocated unevenly to the system three-phases according to Table 2.

5 | RESULTS

In this section, results obtained for the different network operating scenarios and cases of BES characteristics are analysed in terms of load-matching, PV-BES utilization, voltage profiles, power losses and RPF incidents.

5.1 | End-user-oriented analysis

5.1.1 | Load matching assessment

First, the load matching capabilities of the end-users are examined. In Figure 6 the *SCR* variation against PV penetration is presented for all cases and load patterns; both BES CS1 and CS2 are considered. Note that, *SCR* is calculated on annual basis. In general, the use of the BES system improves *SCR*; this is more marked for higher penetration levels. In addition, as PV penetration increases *SCR* decreases, since *B* and *D* of (1) increase accordingly. Comparing CS1 and CS2, it can be realized that *SCR* is higher in the former case. This is attributed to the fact that in CS1 priority is given to the coverage of load demand, resulting into higher amount of selfconsumed energy and consequently to lower PV energy surplus and stored energy in the BES system. Regarding the effect of BES characteristics for CS1, it is shown that for Cases 2 and 3, that is, BES power modification, *SCR* is almost similar to that of the reference Case 1. In addition, *SCR* increases as BES capacity increases (Cases 4 and 5), since higher amount of BES energy is available to cover the load demand. Considering CS2 it can be observed that for low penetration levels *SCR* acquires higher values as the power to energy ratio of BES decreases. On the other hand, for higher penetration levels, for example, >80%, it is shown that *SCR* increases with BES capacity. Similar results have been also obtained for *SSR*, thus are not further analysed.

The annual *LOLP* against PV penetration is plotted in Figures 7(a) and 7(b) for BES CS1 and CS2, respectively, assuming Res. 4. It can be generally seen that *LOLP* is a decreasing function of PV penetration. In particular, considering CS1 the use of BES systems results to lower *LOLP* than that for the PV ADN scenario. This becomes more marked as the BES capacity and/or power increases. Considering CS2, results in Figure 7(b) are not that evident. For low penetration levels, a different behaviour is observed compared to CS1, that is, higher *LOLP* by using BES systems. For Cases 1, 4 and 5, that is, BES systems with power to energy ratio equal to 50%, as the penetration level increases *LOLP* decreases and becomes lower than that for the PV ADN scenario. For Cases 2 and 3 and high penetration levels *LOLP* remains higher than that of the PV ADN; as the power to energy ratio of BES increases *LOLP* acquires higher values than that presented for lower power to energy ratio of BES. From the above analysis, it can be generally concluded that prosumers employing CS2 absorb more often electricity from the grid (higher *LOLP*) compared to PV ADN and CS1 scenarios, since CS2 prioritizes the BES charging process according to the PV production over the load demand. Similar conclusions can be also drawn for load patterns Res. 1–3.

5.1.2 | BES utilization

In Figure 8, *BUI* variation of charging process against PV penetration is examined for different cases of CS1. Similar results emerged for *BUI* variation of discharging process; thus, results are not presented. It is evident that *BUI* is generally an increasing function with PV penetration. Comparing the results of the four load patterns, it can be observed that as PV penetration increases *BUI* curves tend to 80%, regarding Res. 1, 3 and 4; the corresponding *BUI* level for Res. 2 is 70%. For low penetration levels the highest *BUI* is observed for Res. 4. This occurs due to the relatively high misalignment between the load and production profiles, leading to increased BES operation. *BUI* curves for Cases 1 - 3 overlap; for Cases 4 and 5, that is, cases of increased BES capacity, lower values are calculated. This reveals that an increase of the BES power and/or capacity may result into unnecessary investment costs.

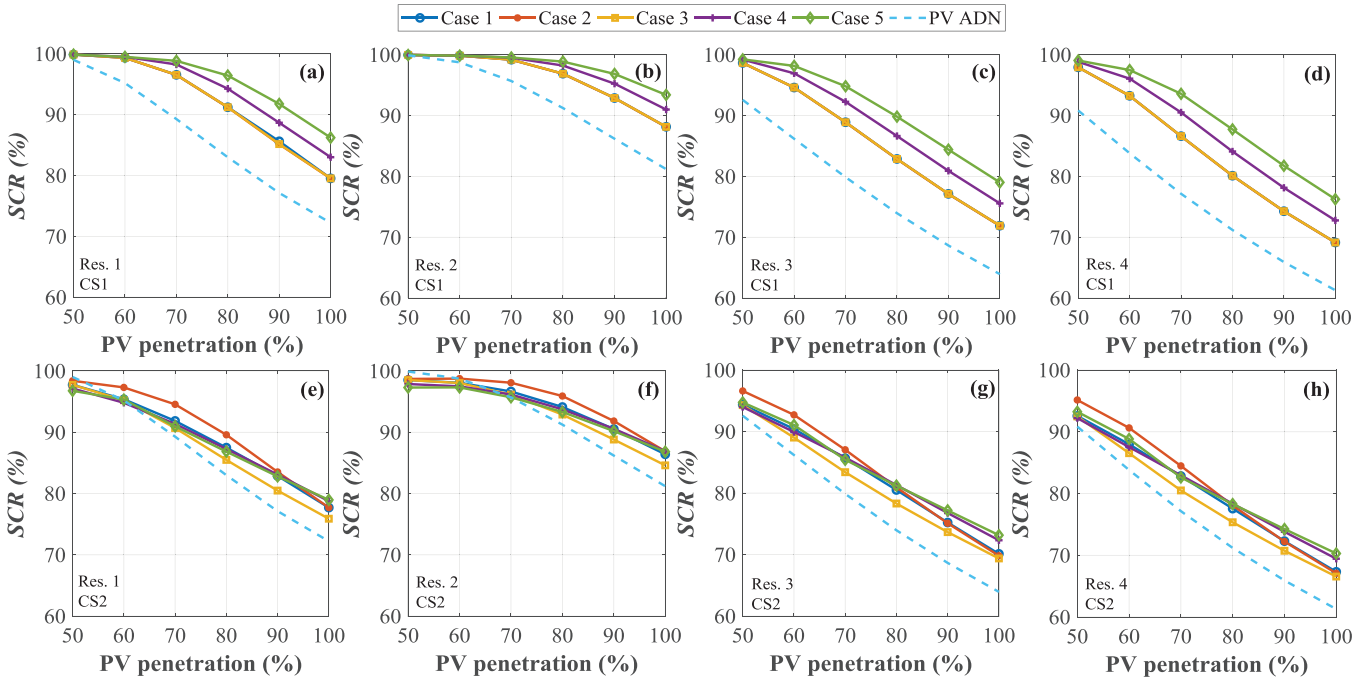

FIGURE 6 SCR against PV penetration for different cases (details are given in each subplot)

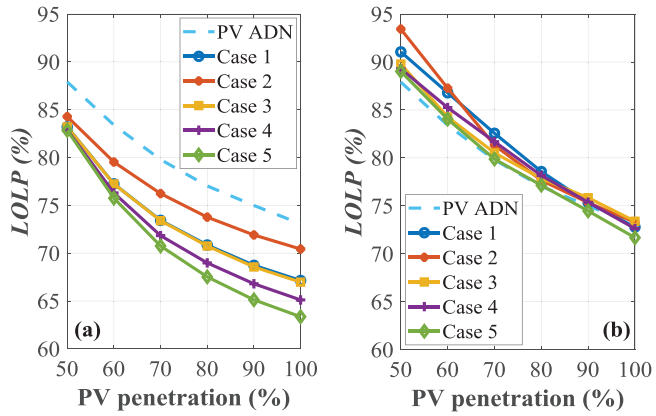

FIGURE 7 LOLP against PV penetration for Res. 4 assuming (a) BES CS1 and (b) BES CS2

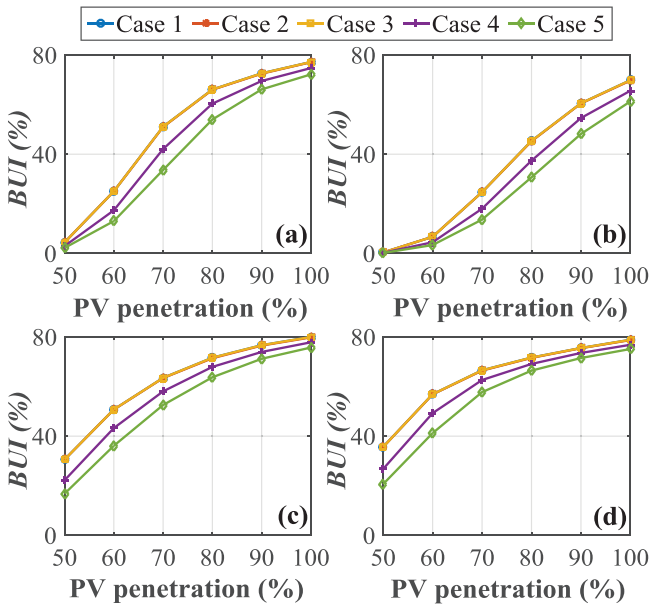

FIGURE 8 BUI (charging process) against PV penetration for (a) Res. 1 (b) Res. 2 (c) Res. 3 (d) Res. 4. BES CS1

BUI variation with PV penetration for BES CS2 is depicted in Figure 9. Similar results are obtained for all load patterns, since under CS2 the BES operation depends only on the PV production. It is shown that for Cases 1 and 2, *BUI* remains constant against PV penetration, acquiring values equal to ∼64% and 59%, respectively. Comparing these cases, it can be deduced that BES power reduction by 50% results only into a slight *BUI* decrease (5%). For Cases 3, 4 and 5, the same behaviour is observed as for BES CS1.

From the comparative assessment of the *BUI* results regarding BES CS1 and CS2, it can be concluded that for low penetration levels higher BES utilization is achieved under BES CS2; the opposite behaviour is observed as PV penetration increases.

Finally, indicative results of the capacity degradation of BES CS1 and CS2 with PV penetration are presented in Figures 10(a) and 10(b), respectively. Owing to annual analysis, the formation of the solid electrolyte interphase occurred at the early operating cycles of BES has a strong impact on capacity degradation. For this reason, the acquired $capd^{l}$ is in the range of 4.5% to 6.5% (considered relatively high). Also, it can be realized that the results of Figures 10(a) and 10(b) present a similar trend as those of Figures 8(d) and 9, respectively. This implies that there is a strong correlation between BES utilization and capacity

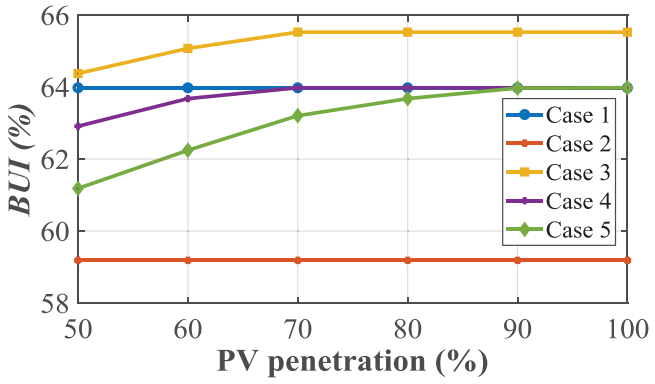

FIGURE 9 BUI (charging process) against PV penetration for BES CS2

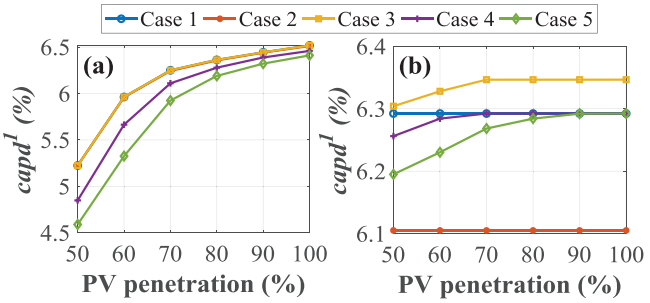

FIGURE 10 capd[1] against PV penetration for Res. 4 (a) BES CS1 (b) BES CS2

degradation, that is, higher BES utilization leads to higher BES capacity degradation.

5.2 | Network-oriented analysis

5.2.1 | Voltage assessment

The voltage performance of the overall network is evaluated by means of CDF plots. The CDF random variable is the voltage magnitude results of L_1L_{11}. PV ADN and PV-BES ADN operation (Case 1) are compared, considering different PV penetration levels. In all simulations Res. 4 load pattern is employed and the resulting CDFs are summarized in Figure 11. As expected, the voltage rise probability increases with PV penetration level due to the increased reverse power flow. However, BES utilization improves the ADN voltage profiles. This can be justified by the fact that the use of BES reduces the amount of the reverse power flowing to the grid during high production periods. Similar remarks are also concluded for load patterns Res. 1–3.

The overall system voltage performance is also examined by calculating *VLQI*. The *VLQI* of the annual network voltages against PV penetration is plotted in Figure 12 considering different cases; results are presented for the four load patterns. It is shown that for low penetration levels, *VLQI* acquires lower values for CS2 compared to CS1; as PV penetration increases, CS2 results into higher voltage rise. Additionally, for cases of

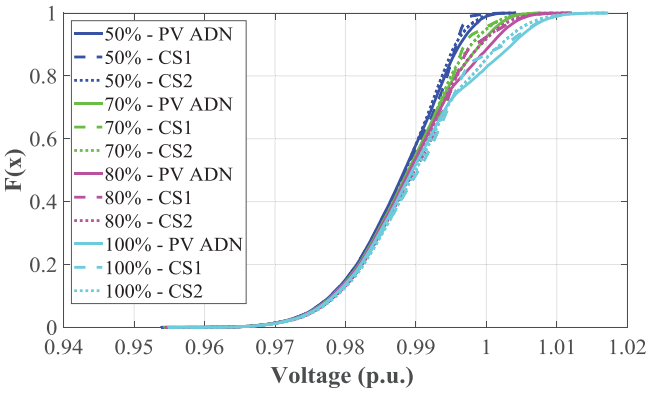

FIGURE 11 CDF for varying PV penetration level

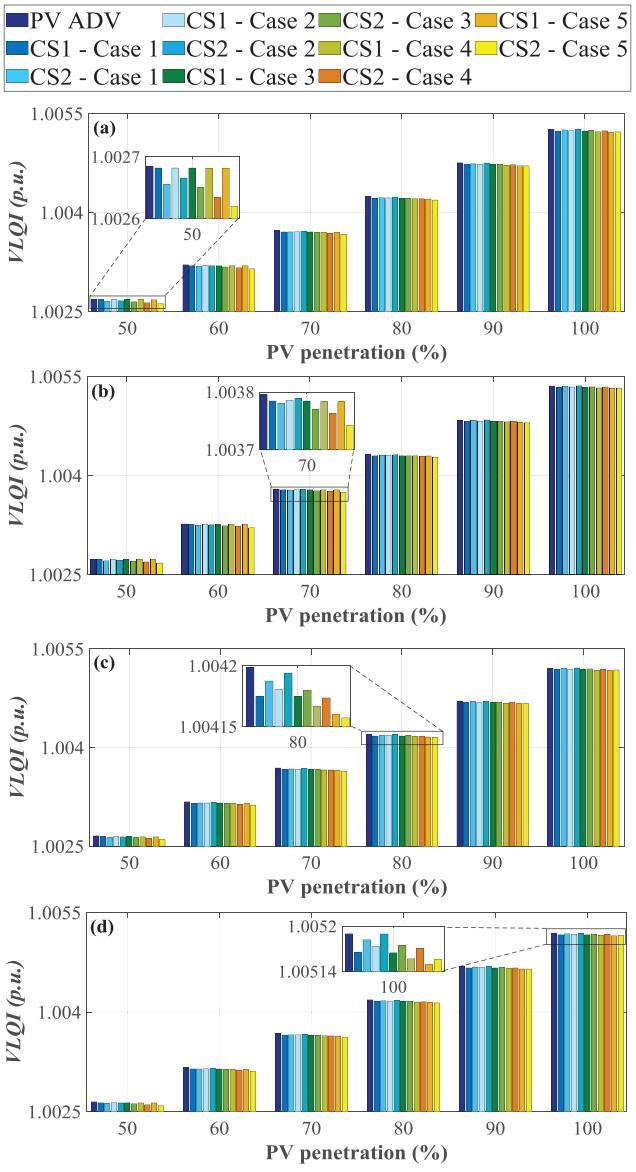

FIGURE 12 VLQI against PV penetration for (a) Res. 1, (b) Res. 2, (c) Res. 3, (d) Res. 4

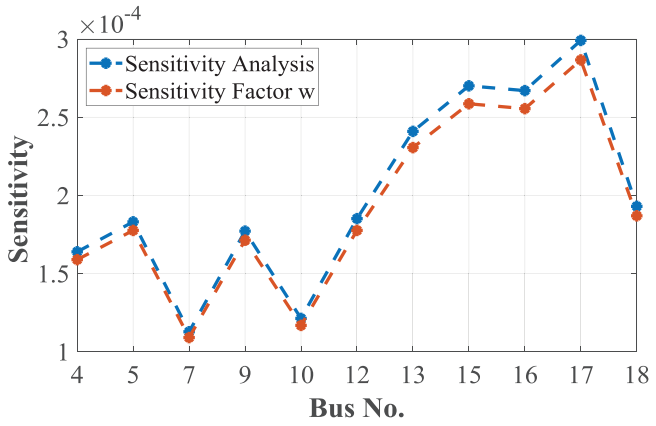

FIGURE 13 Sensitivity of load buses for Res. 4 (passive network)

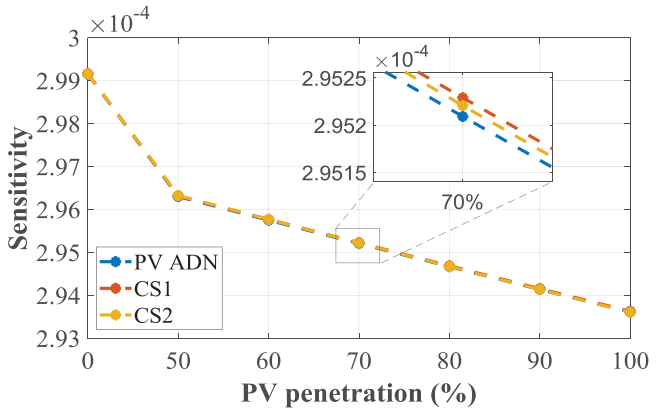

FIGURE 14 Sensitivity of Bus No. 17 against PV penetration for Res. 4 (Case 1)

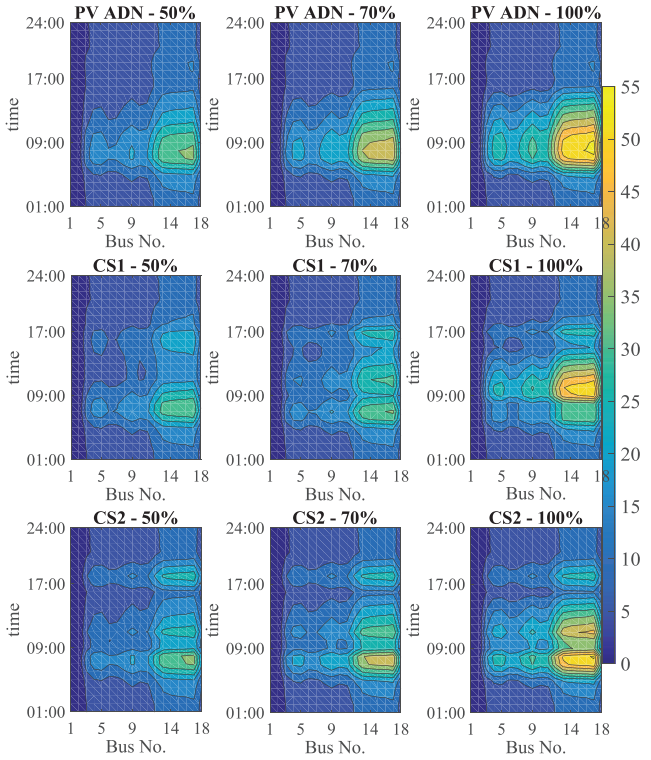

FIGURE 15 Voltage variance of buses for Res. 4 (Case 1)

decreased BES power, that is, Case 2, *VLQI* becomes higher compared to reference Case 1. On the contrary, *VLQI* decreases with increasing BES capacity and power, that is, Cases 3–5; this is evident for both BES strategies. This can be justified by the fact that the increased BES capacity and power provides an additional flexibility to the grid, leading to reduced network voltages, since the reverse power flow is decreased during high production periods.

In addition, the simplified and the exact approaches for the calculation of w_n are compared in Figure 13. Note that, load pattern Res. 4 is considered. Similar results are obtained by using the two approaches. Differences between the simplified and the exact approach are in the range of 1.69% to 2.43%. Note that, the lowest difference is observed for bus No. 7, that is, the bus presenting the lowest sensitivity. On the other hand, bus No. 17, that is, the most distant bus of the feeder, presents the highest sensitivity to voltage against active power changes as well as the highest difference. The sensitivity of this bus is further analysed in Figure 14 for different operating scenarios. It can be realized that w_n is a decreasing function against PV penetration. In addition, it is not significantly affected by BES systems. Similar remarks are derived also for load patterns Res. 1–3.

The voltage sensitivity is also examined by using $\sigma^2_{n,b}$. Results for all network buses are illustrated in Figure 15, by using colour maps. PV-BES ADN (CS1 and CS2) as well as PV ADN operation are considered, assuming load pattern Res. 4 and 50%, 70% and 100% PV penetration. As expected, significant voltage variation is observed for all cases at bus No. 17. It can be also realized that voltage variations are more often during the day for PV-BES ADN operation; this is more evident for CS2. Lower $\sigma^2_{n,b}$ is observed when CS1 applies, resulting into smoother voltage profiles compared to CS2.

Finally, in order to investigate voltage unbalance the load allocation of Table 2 is assumed for all end-users. The obtained annual VUF_0 and VUF_2 results are averaged and plotted against PV penetration in Figures 16 and 17, respectively. Different load patterns and operating scenarios (PV ADN, CS1 and CS2) are examined, assuming BES characteristics of Case 1. In general, Res. 2 pattern results into the highest VUF_0 and VUF_2, while Res. 4 into the lowest ones. The use of three-phase PV-BES systems practically does influence the voltage unbalance; in fact, no voltage mitigation technique has been used. Specifically, considering maximum PV penetration, VUF_0 and VUF_2 is improved only by 2% and 4.5%, respectively. The overlapping VUF_0 and VUF_2 curves for the three operating scenarios are also attributed to the lack of voltage mitigation technique application. The slight differences are due to deviations in the active power flows, influencing the positive-sequence voltage and consequently the calculation of VUF_0 and VUF_2 by means of (11) and (12), respectively.

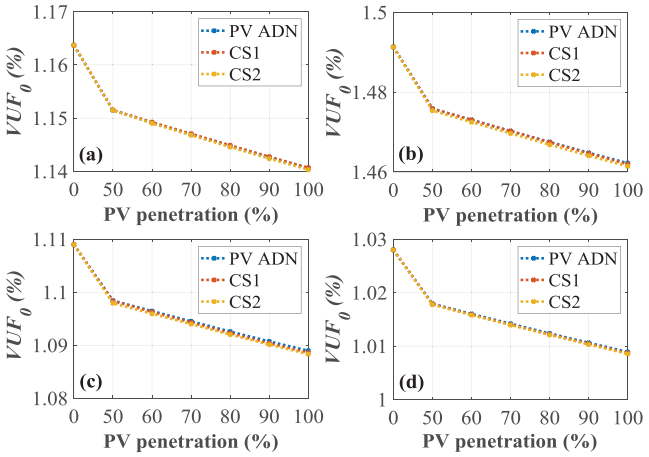

FIGURE 16 VUF_0 against PV penetration for (a) Res. 1 (b) Res. 2 (c) Res. 3 (d) Res. 4. (Case 1)

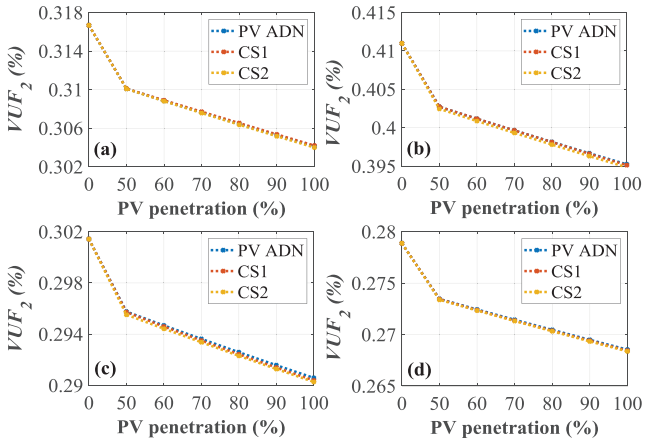

FIGURE 17 VUF_2 against PV penetration for (a) Res. 1 (b) Res. 2 (c) Res. 3 (d) Res. 4. (Case 1)

5.2.2 | Power losses evaluation

System losses are evaluated by investigating the *LRI* variation against PV penetration in Figure 18 for different cases. Results generally reveal that system losses are mostly affected by CS1, since in this case they are an increasing function of PV penetration. On the other hand, regarding CS2 *LRI* results are practically unaffected. For low penetration levels, the *LRI* acquires higher values for CS2 than CS1. This is due to the more often use of the BES system in CS2, resulting consequently into higher BES losses. The opposite behaviour is observed for higher penetration levels, for example, >80%. Regarding the effect of BES characteristics, it is shown that for Cases 2 and 3, that is, BES power modification from reference Case 1, *LRI* is similar to that of Case 1; this is evident for both BES strategies. However, for Cases 4 and 5 *LRI* acquires higher values, especially with increasing PV penetration. The reason behind this lies on the use of a BES with increased installed capacity and maximum output power. More specifically, this type of BES can handle larger amounts of energy during the day. Thus, the corresponding BES losses are significantly increased leading to higher values of *LRI*. Similar results as above can be concluded for *LLR*, thus results are not presented.

In Figure 19 the total system losses are decomposed to distribution line (left *y*-axis) and BES (right *y*-axis) losses. Their variation against PV penetration is analysed for Case 1, assuming load patterns Res. 1–4. Line losses for patterns Res. 1, 3 and 4 decrease up to a certain value of the penetration level; above this value line losses start to increase, due to reverse power flow as a result of energy excess from prosumers. On the other hand, line losses for load pattern Res. 2 is a decreasing function of PV penetration. Annual line losses can be also evaluated in monetary terms; thus the results of Figure 19 correspond to a cost from 388.84€ to 813.93€ considering the tariffs of the Greek electricity market [38]. Also, comparing PV-BES ADN and PV ADN operation it can be observed that PV-BES operation results into reduced line losses, especially when CS2 is applied; the corresponding profit ranges from 10.13€ to 52.68€ per year. Contrary to CS1, in CS2, the BES charges only for high levels of PV production, absorbing the surplus energy and preventing it from being injected into the grid which causes additional losses. From Figure 19 it can be also deduced that the annual line and the corresponding BES losses can be generally regarded comparable.

It should be indicated that BES system losses analysis provides information concerning the end-user; thus, can be directly associated to the corresponding *BUI* investigations. For example, the increased BES losses in CS1 to CS2 correspond to higher *BUI* results in Figure 8.

5.2.3 | RPF analysis

The variation of the active power flow at the secondary of the distribution transformer (P_{TF}) between operating scenarios is compared by means of Q-Q plots, identifying possible RPF incidents. In Figure 20 CS1 and CS2 are compared for different PV penetration levels. Note that, P_{TF} lower than zero indicates RPF from the LV ADN to the upstream MV network. As expected, more RPF incidents occur as the PV penetration increases (more cases of active power flow with negative value). From this figure it can be also inferred that CS2 leads to more RPF incidents compared to CS1. This is attributed to the fact that there are more occurrences of PV production and load matching ($P_{TF} \approx 0$ kW) for CS1 than for CS2.

Next, the impact of load profiles on P_{TF} is examined in Figure 21 for different scenarios (details are given on the figure); Res. 2 and Res. 4 are compared, corresponding to the highest and lowest average demand from the examined load patterns. For CS1 (see Figures 21(a) and 21(c)) more RPF incidents occur when Res. 4 is considered instead of Res. 2. However, for CS2 similar results are obtained for the two cases (Figures 21(b) and 21(d)); P_{TF} is slightly influenced by the prosumer's profile pattern, since under CS2 the charging and discharging process of the BES system is mainly influenced by the PV production profile.

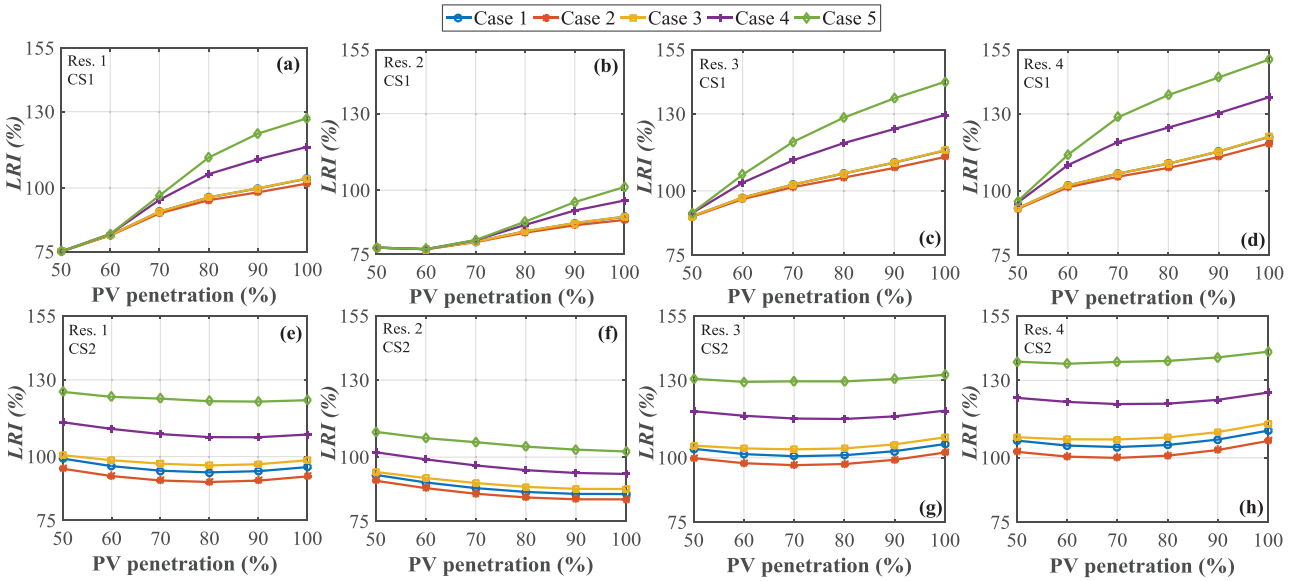

FIGURE 18 LRI against PV penetration for different cases

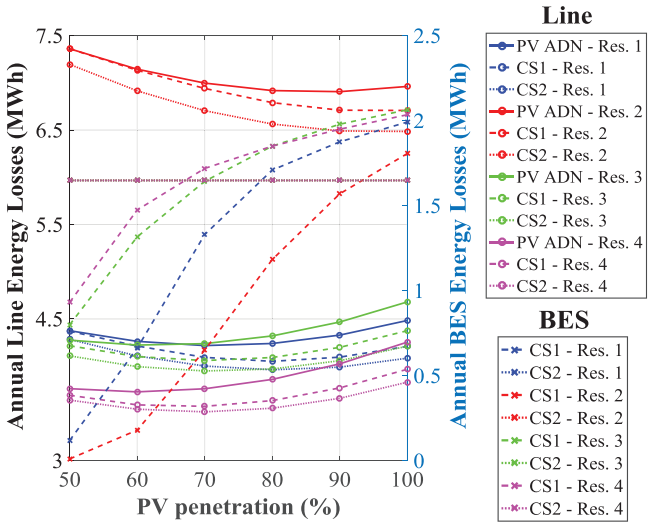

FIGURE 19 Annual grid and BES energy losses with PV penetration (Case 1)

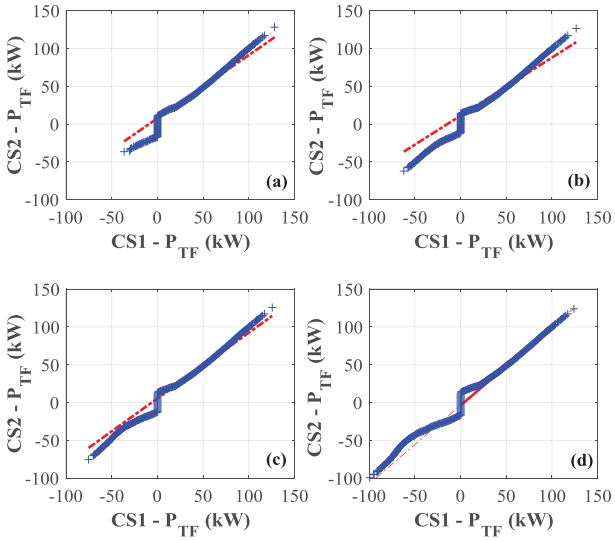

FIGURE 20 Q-Q plot of P_{TF} between CS1 and CS2 for PV penetration level (a) 50%, (b) 70%, (c) 80% and (d) 100% for Res. 4 (Case 1)

Finally, in Figures 22 and 23 the impact of BES characteristics on P_{TF} is investigated for CS1 and CS2, respectively. Res. 4 and PV penetration equal to 80% are considered. For CS1, more RPF incidents occur for decreased BES power, that is, Case 2 (Figure 22(a)). By increasing the BES power, that is, Case 3, the comparison with Case 1 in Figure 22(b) shows that the corresponding P_{TF} results practically overlap, since BES utilization is similar for these cases (see *BUI* in Figure 8(d)). From Figures 22(c) and 22(d), it can be deduced that BES systems with higher capacity, that is, Cases 4 and 5 result in less RPF incidents. On the other hand, for CS2 generally linear Q-Q plots are derived in Figure 23. This reveals that P_{TF} and consequently RPF incidents are not practically influenced by the BES characteristics. Small differences are attributed to the different BES utilization as also indicated by the corresponding *BUI* results (see Figure 9).

Regarding the reactive power flow at the distribution transformer, the comparison of the examined scenarios leads to linear Q–Q plots, since no reactive power control is employed in this analysis; thus, the corresponding results are not presented. It should be also indicated that, all the above remarks are also concluded for load patterns Res. 1–3.

6 | CONCLUSION

A generalized framework for the probabilistic performance assessment of LV ADNs with PV-BES systems is proposed in

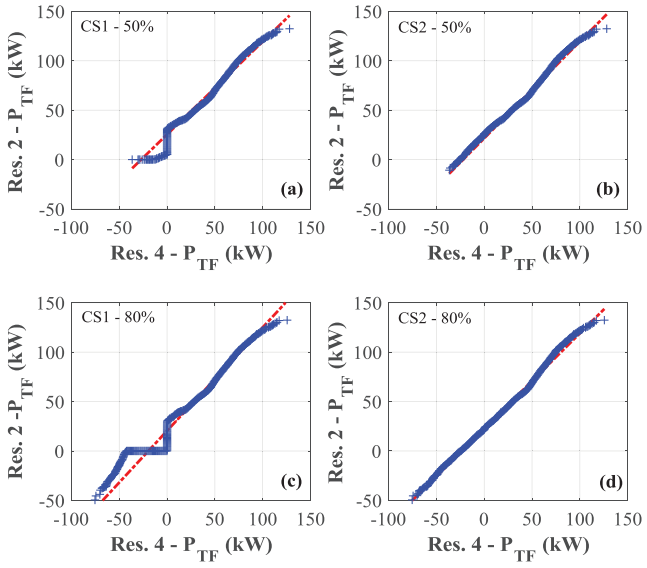

FIGURE 21 Q-Q plot of P_{TF} between Res. 4 and Res. 2 for different BES control strategies and PV penetration levels (α) CS1 - 50%, (b) CS2 - 50%, (c) CS1 - 80% and (d) CS2 - 80% (Case 1)

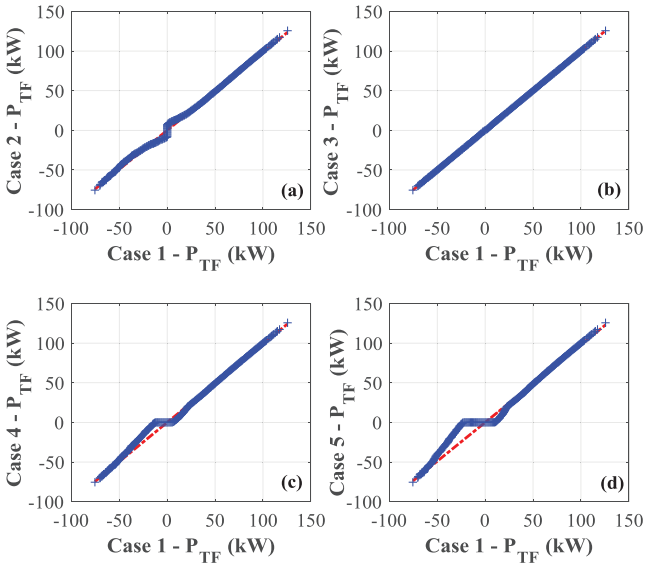

FIGURE 22 Q-Q plot of CS1 P_{TF} results. Comparison between Case 1 and (a) Case 2, (b) Case 3, (c) Case 4, (d) Case 5

this paper. The proposed framework is considered generalized in the sense that it can be applied to any network configuration and incorporate any type of PV and/or BES control schemes, centralized or decentralized optimization techniques etc. Time-series power flow calculations are conducted on annual basis and results are statistically analysed considering a wide range of operating conditions and test cases. A set of probabilistic indices is developed, consisting of already known or newly introduced in this work, and a BES capacity degradation model is employed to evaluate the impact of PV-BES systems on the performance of individual end-users as well as of the overall network.

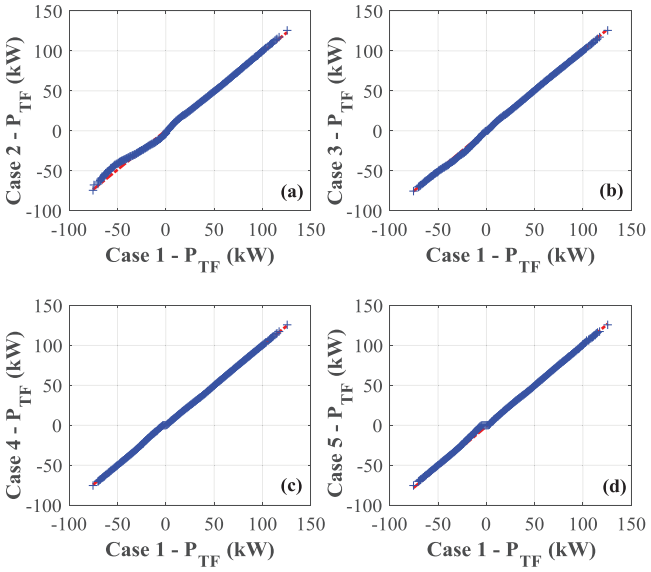

FIGURE 23 Q-Q plot of CS2 P_{TF} results. Comparison between Case 1 and (a) Case 2, (b) Case 3, (c) Case 4, (d) Case 5

The application of the proposed framework to a LV ADN has shown that defined indices *SCR*, *SSR* and *LOLP* can be used to evaluate the onsite production share of the PV-BES system on the local demand of end-users. Furthermore, to assess the BES system applicability a new index has been introduced, namely *BUI*. In addition, the employment of a BES degradation model has shown that there is a strong correlation between BES utilization and BES aging. Specifically, it has been verified that lower BES utilization, that is, lower values of *BUI*, leads to decelerated cyclic aging of BES and subsequently in calendar life expansion.

Network-oriented analysis demonstrated that the proposed probabilistic voltage assessment method can assist the evaluation of voltage levels and indicate the most proper operating scenario in terms of voltage profile improvement. Preliminary analysis of voltage sensitivity is conducted by using sensitivity factor w_n. Results indicate that accurate estimates of w_n are obtained by using a simplified and computational efficient approach. In this context, the developed voltage variance index can also help distribution system operators to identify and verify the most sensitive buses to voltage variations; this enables them to take measures regarding the system limits. In general, it has been observed that the increasing penetration of PV units leads to increased voltage levels. This issue is settled by BES utilization leading to improved voltage profiles as well as decreased voltage levels. Moreover, voltage unbalance has been examined by adopting the VUF_0 and VUF_2 indices. Both negative and zero sequence voltage unbalances are strongly influenced by the load pattern profile. *LRI* and *LLR* indices have been adopted to determine the optimal PV penetration level in order to achieve minimum system losses. According to the obtained results, a general trend can be identified for line losses behaviour. Specifically, line losses decrease up to a certain value of the PV penetration level, while above this value line losses start to increase, due to reverse power flow. The exact value of the PV

penetration level minimizing line losses is depended on various parameters, for example, the examined network configuration, load/production profiles of end-users etc. In addition, it has been observed that the employment of BES by LV prosumers leads to further decrease of the overall network losses. However, it is also worth noting that annual BES losses can be comparable to distribution line losses; thus, must be taken into account in the analysis. Finally, RPF incidents at the distribution substation were graphically identified by means of Q-Q plots.

A systematic step-by-step procedure to assess in a probabilistic manner the performance of all network assets and identify underlying tendencies has been introduced. The proposed framework can constitute a useful tool to distribution system operators to coordinate further their operation and take future mutually beneficial corrective measures. In addition, end-users can analyse their load-matching behaviour and investigate their capability to achieve higher financial benefits and provide ancillary services to the network, especially, if participate in the energy market by employing special trading models, for example, peer-to-peer trading.

Finally, it should be indicated that the proposed framework can be also applied in terms of Monte Carlo simulations to take into account system uncertainties, for example, in load/generation. Moreover, it can be extended to evaluate the economic impact of PV-BES systems, considering specific electricity policies and thus contribute further to the better understanding of their effect in modern LV networks.

ACKNOWLEDGEMENTS

The research work was supported by the Hellenic Foundation for Research and Innovation (H.F.R.I.) under the "First Call for H.F.R.I. Research Projects to support Faculty members and Researchers and the procurement of high-cost research equipment grant" (Project Number: HFRI-FM17-229).

DATA AVAILABILITY STATEMENT

The data that support the findings of this study are openly available at https://activate.ee.duth.gr/downloads/, reference number [29].

CONFLICT OF INTEREST

The authors declare no conflict of interest.

ORCID

Kalliopi D. Pippi https://orcid.org/0000-0002-0931-284X
Theofilos A. Papadopoulos https://orcid.org/0000-0001-6384-1964

REFERENCES

1. Olivares, D.E., Mehrizi-Sani, A., Etemadi, A.H., et al.: Trends in microgrid control. IEEE Trans. Smart Grid 5(4), 1905–1919 (2014)
2. CIGRE WG C4.605 report, modelling and aggregation of loads in flexible power networks
3. Chowdhury, B.H., Sawab, A.W.: Evaluating the value of distributed photovo1aic generations in radial distribution systems. IEEE Trans. Energy Convers. 11(3), 595–600 (2013)
4. Srisaen, N. & Sangswang, A.: Effects of PV grid-connected system location on a distribution system. In: Procedings of IEEE Asia Pacific Conference on Circuits and Systems, pp. 852–855. IEEE, Piscataway (2006)
5. Sukumar, S., Mokhlis, H., Mekhilef, S., et al.: Ramp-rate control approach based on dynamic smoothing parameter to mitigate solar PV output fluctuations. Int. J. Electr. Power Energy Syst. 96, 296–305 (2018)
6. Kryonidis, G.C., Kontis, E.O., Chrysochos, A.I., et al.: A coordinated droop control strategy for overvoltage mitigation in active distribution networks. IEEE Trans. Smart Grid 9(5), 5260–5270 (2018)
7. Nousdilis, A.I., Christoforidis, G.C., Papagiannis, G.K.: Active power management in low voltage networks with high photovoltaics penetration based on prosumers' self-consumption. Appl. Energy 229, 614–624 (2018)
8. Robak, S., MacHowski, J., Gryszpanowicz, K.: Automatic alleviation of overloads in transmission network by generation curtailment. IEEE Trans. Power Syst. 33(4), 4424–4432 (2018)
9. Chiradeja, P., Ramakumar, R.: An approach to quantify the technical benefits of distributed generation. IEEE Trans. Energy Convers. 19(4), 764–773 (2004)
10. Hasheminamin, M., Agelidis, V.G., Salehi, V., et al.: Index-based assessment of voltage rise and reverse power flow phenomena in a distribution feeder under high PV penetration. IEEE J. Photovoltaics 5(4), 1158–1168 (2015)
11. Tévar-Bartolomé, G., Gómez-Expósito, A., Arcos-Vargas, A., et al.: Network impact of increasing distributed PV hosting: A utility-scale case study. Sol. Energy 217, 173–186 (2021)
12. Verbruggen, B., Driesen, J.: Grid impact indicators for active building simulations. IEEE Trans. Sustain. Energy 6(1), 43–50 (2015)
13. Gjorgievski, V., Cundeva, S.: The effects of residential battery storage on grid impact indicators. In: 2019 IEEE Milan PowerTech. IEEE, Piscataway (2019)
14. Tan, X., Li, Q., Wang, H.: Advances and trends of energy storage technology in Microgrid. Int. J. Electr. Power Energy Syst. 44(1), 179–191 (2013)
15. Li, X., Wang, S.: A review on energy management, operation control and application methods for grid battery energy storage systems. CSEE J. Power Energy Syst. 7(5), 1026–1040 (2019)
16. Davidson, I.E., Reddy, R.: Performance evaluation of solar roof-top PV on Eskom's LV electric power distribution networks. In: 2019 7th International Conference on Smart Grid (icSmartGrid), pp. 97–102. IEEE, Piscataway (2019)
17. Shaw-Williams, D., Susilawati, C., Walker, G., et al.: Valuing the impact of residential photovoltaics and batteries on network electricity losses: An Australian case study. Utilities Policy 60, 100955 (2019),
18. Gjorgievski, V., Cundeva, S.: Implications of residential battery charge and discharge rates on self-consumption and peak power exchange. In: 2019 16th Conference on Electrical Machines, Drives and Power Systems (ELMA), pp. 1–5. IEEE, Piscataway (2019)
19. Katsanevakis, M., Stewart, R.A., Junwei, L.: A novel voltage stability and quality index demonstrated on a low voltage distribution network with multifunctional energy storage systems. Electr. Power Syst. Res. 171, 264–282 (2019)
20. Vanin, A., Ellina, S., Nardelli, P.J., et al.: Dispatch optimization of energy communities for collective provision of network congestion management. In: 2021 3rd International Youth Conference on Radio Electronics, Electrical and Power Engineering (REEPE), pp. 1–5. IEEE, Piscataway (2021)
21. Pippi, K.D., Papadopoulos, T.A., Kryonidis, G.C.: Impact assessment framework of PV-BES systems to active distribution networks. In: Mediterranean Conference on Power Generation, Transmission, Distribution and Energy Conversion (MedPower 2020). IEEE, Piscataway (2020)
22. Gjorgievski, V.Z., Chatzigeorgiou, N.G., Venizelou, V., et al.: Evaluation of load matching indicators in residential PV systems-the case of cyprus. Energies 13(8), 1934 (2020)
23. Barzegkar-Ntovom, G.A., Kontis, E.O., Kryonidis, G.C., et al.: Performance assessment of electrical storage on prosumers via pilot case studies. In: 2019 1st International Conference on Energy Transition in the Mediterranean Area (SyNERGY MED), pp. 1–6.(2019)
24. Brenna, M., De Berardinis, E., Carpini, L.D., et al.: Automatic distributed voltage control algorithm in smart grids applications. IEEE Trans. Smart Grid 4(2), 877–885 (2013)
25. Kontis, E.O., Kryonidis, G.C., Nousdilis, A.I., et al.: A two-layer control strategy for voltage regulation of active unbalanced LV distribution networks. Int. J. Electr. Power Energy Syst. 111, 216–230 (2019)

26. Alam, M.J.E., Muttaqi, K.M., Sutanto, D.: An approach for online assessment of rooftop solar PV impacts on low-voltage distribution networks. IEEE Trans. Sustain. Energy 5(2), 663–672 (2014)
27. Papadopoulos, P.N., Milanović, J.V.: Probabilistic framework for transient stability assessment of power systems with high penetration of renewable generation. IEEE Trans. Power Syst. 32(4), 3078–3088 (2017)
28. ACTIVATE: https://activate.ee.duth.gr/downloads
29. Dugan, R.C., Montenegro, D.: Reference guide: The Open Distribution System Simulator.Tech. Rep. 9.0.0. Electrical Power Research Institute, Washington, DC (2020)
30. Nousdilis, A.I., Chrysochos, A.I., Papagiannis, G.K., et al.: The impact of photovoltaic self-consumption rate on voltage levels in LV distribution grids. In: IEEE International Conference on Compatibility, Power Electronics and Power Engineering, pp. 650–655. IEEE, Piscataway (2017)
31. Pfenninger, S., Staffell, I.: Renewables ninja. https://www.renewables.ninja/. Accessed December 2019
32. Nousdilis, A.I., Kryonidis, G.C., Kontis, E.O., et al.: Impact of policy incentives on the promotion of integrated PV and battery storage systems: A techno-economic assessment. IET Renew. Power Gener. 14(7), 1174–1183 (2020)
33. Nieslony, A.: Rainflow counting algorithm. https://de.mathworks.com/matlabcentral/fileexchange/3026-rainflow-counting-algorithm. Assessed 8 September 2021
34. Siano, P., Mohammad, D.: MILP Optimization model for assessing the participation of distributed residential PV-battery systems in ancillary services market. CSEE J. Power Energy Syst. 7(2), 348–357 (2021)
35. Dolatabadi, M., Siano, P.: A scalable privacy preserving distributed parallel optimization for a large-scale aggregation of prosumers with residential PV-battery systems. IEEE Access 8, 210950–210960 (2020)
36. Celik, B., Suryanarayanan, S., Roche, R., et al.: Quantifying the impact of solar photovoltaic and energy storage assets on the performance of a residential energy aggregator. IEEE Trans. Sustain. Energy 11(1), 405–414 (2020)
37. Stetz, T., Marten, F., Braun, M.: Improved low voltage grid-integration of photovoltaic systems in germany. IEEE Trans. Sustain. Energy 4(2), 534–542 (2012)
38. Energy Exchange Group (EnEx): https://www.enexgroup.gr/el/web/guest/home. Assessed 8 September 2021

How to cite this article: Pippi, K. D., Papadopoulos, T. A., Kryonidis, G. C.: Impact assessment framework of PV-BES systems to active distribution networks. IET Renew. Power Gener. 16, 33–47 (2022). https://doi.org/10.1049/rpg2.12313